# Regularized Simultaneous Super-Resolution with Automatic Determination of the Parameters


Marcelo V. W. Zibetti, Joceli Mayer *
Federal University of Santa Catarina
Department of Electrical Engineering
Florianópolis, Brazil

Fermín S. V. Bazan
Federal University of Santa Catarina
Department of Mathematics
Florianópolis, Brazil



## Abstract

*We derive a novel method for automatic determination of the regularization parameters applicable for the class of simultaneous super-resolution (SR) algorithms. The proposed method is based on the classical joint maximum a posteriori (JMAP) estimation technique, which is a fast alternative to estimate the parameters. Unfortunately, the classical JMAP technique can be unstable and generates multiple local minima. In order to stabilize the JMAP estimation, while achieving a cost function with a unique global solution, we derive an improved solution by modeling the JMAP hyperparameters with a gamma prior distribution. Experimental results illustrate the effectiveness of the proposed method for automatic determination of the regularization parameters for the simultaneous SR. We also contrast the proposed method to a reference method named KNOWN. KNOWN is a MAP based simultaneous SR algorithm where the parameters are fixed, either known a priori or extracted from the high-resolution frames which are not usually available in practice.*


## 1. Introduction

In many applications it is required that the acquisition system provides an image with the best possible resolution, while introducing minimum distortions due to imperfections of the image sensor and the optical system. However, the cost of image acquisition systems, like digital cameras, camcorders and scanners, increases with the resolution of the sensor and with the quality of the optical system. An alternative to improve the resolution and the quality of captured images, without increasing the cost of the system, is to employ digital processing techniques to achieve super-resolution (SR).

Research on super-resolution (SR) algorithms began in the 90's. One of the pioneering works, in [25], employed Fourier domain methods. Since then, different approaches have been developed, including projections onto convex sets (POCS), non-uniform interpolation and iterative back-projection, as reviewed by [18]. Regularized SR approaches based on maximum a posteriori (MAP) and regularized least squares appeared in [21, 12]. Traditionally, regularized approaches minimize a cost function composed by the residual associated with the estimated high-resolution (HR) frame plus another term, called the prior term, used to regularize the problem. In these approaches, the regularization parameter scales the influence of the prior term in the resulting solution. In most SR methods, the parameter is assumed to be known by some way. In the majority of practical cases, the parameter as well as the HR images must be estimated from the data.

In *simultaneous* SR methods, proposed in [4, 28, 29, 30], all frames of an image sequence are estimated in a single process. Two different kinds of priors are employed, one to achieve spatial smoothness and other to achieve higher similarity of the HR frames in the motion trajectory. In these problems at least two parameters are necessary, and to the best of our knowledge, a proper method to find the regularization parameters for these techniques has not been proposed yet.

In this paper we address the problem with two parameters in the simultaneous SR. Section 2 provides a detailed description of system models used in this work. The simultaneous SR algorithm with fixed regularization parameters is reviewed in Section 2.2. In Section 3, the new method with automatic determination of the parameters is proposed using the joint maximum a posteriori (JMAP) estimation technique [8]. The classical JMAP approach, which assumes uniform density for the hyperparameters is, in general, unstable [8]. To circumvent this, we assume a gamma probability density for the hyperparameters which results in


* This research is sponsored by CNPq grants: 140543/2003-1 300487/94 - 0(NV), 472536/2007-9 (e-mails: marcelo.zibetti@terra.com.br, fermin@mtm.ufsc.br, mayer@eel.ufsc.br).

a stable algorithm with a unique global solution. Section 4 presents experiments, comparisons and discussions to illustrate the performance. Section 5 concludes this paper.

## 2. Review of the System Models and the Simultaneous SR Methods with Fixed Parameters

This section describes the models adopted in the super-resolution algorithms and presents the simultaneous super-resolution algorithm with fixed parameters.

### 2.1. System Models Used in Super-Resolution

The models adopted in the simultaneous super-resolution algorithms are: acquisition model, motion model, and the image model.

**2.1.1. Acquisition Model** This model describes the transformations imposed to the images during the acquisition process. In this model, the observed data are the low-resolution images. The model is described in the following equation:

$$\mathbf{g}_k = \mathbf{D}_k \mathbf{f}_k + \boldsymbol{\eta}_k \tag{1}$$

where $\mathbf{g}_k$ is a vector, of size $N \times 1$, that represents the LR frame captured at the instant $k$. The elements of the vector $\mathbf{g}_k$ correspond to the pixels of the LR frame, lexicographically ordered. The size $N = N_1 N_2$ is the number of pixels, where $N_1 \times N_2$ is the size of the LR frame in the horizontal and vertical directions, respectively. The vector $\mathbf{f}_k$, of size $M \times 1$, represents the HR image, of size $M_1 \times M_2$, with $M = M_1 M_2$ pixels ordered lexicographically, where $N \leq M$. The vector $\boldsymbol{\eta}_k$ represents acquisition noise, which is usually assumed to be i.i.d. with normal distribution and presenting the same variance $\sigma^2_{\boldsymbol{\eta}}$ for all frames. The matrix $\mathbf{D}_k$, of size $N \times M$, represents the acquisition transformation applied to the HR image $\mathbf{f}_k$. It models the distortions due to the optics imperfections and to the subsampling, which reduces the number of pixels from the HR frame to the LR frame.

**2.1.2. Motion Model** This model describes the transformations caused by the relative motion among objects in the frames of the sequence. It assumes that the frame in the temporal instant $k$ can be represented by the frame in the temporal instant $j$, with the motion compensated, plus a new information $\mathbf{e}_{k,j}$, which cannot be obtained from the frame in the instant $j$. The equation that describes the model is:

$$\mathbf{f}_k = \mathbf{M}_{k,j} \mathbf{f}_j + \mathbf{e}_{k,j} \tag{2}$$

where $\mathbf{f}_k$ and $\mathbf{f}_j$ are vectors that represent the frames in the temporal instants $k$ and $j$, respectively. The matrix $\mathbf{M}_{k,j}$, of size $M \times M$, represents the motion transformation, or warping. This matrix is usually very sparse [19]. Most of the elements in an arbitrary line $m$ are equal to zero, except for: 1) one element with unitary value, in the column $n$, that represents the displacement of the pixel $n$ in $\mathbf{f}_j$ to the position $m$ in $\mathbf{f}_k$; 2) a few non-zero elements, which corresponds to the linear combination of determined pixels (interpolation) of $\mathbf{f}_j$ to generate the pixel $m$ in $\mathbf{f}_k$. This occurs due to sub-pixel displacements in the high-resolution grid.

The matrix $\mathbf{M}_{k,j}$ can be created either from a discretized continuous motion operator [2, 1], where a parametric motion is assumed, or from a discrete motion vector field [24, 20]. The vector $\mathbf{e}_{k,j}$, also called motion error, is the new information in the frame $k$ that cannot be obtained from the frame in the instant $j$. This new information is usually originated by small errors in the estimation of the motion parameters, by limitations of the discretized motion operator in properly representing the continuous motion, or by *outliers*[1]. In the context of motion, an outlier is usually a region or an object that has been occluded by another object or due to objects that suddenly appear in the scene or regions that suffered unexpected motion [11].

It is important to notice that the outliers cause distortions in the HR image estimation. In order to avoid these distortions, a detection and removal procedure [20, 4] or an outlier robust SR algorithm [9, 29, 30] can be employed. Another approach to reduce these distortions is to control the parameters related to the similarity of the images in the motion trajectory. This work evaluates the performance of the parameter determination methods in finding the proper values to reduce the distortions caused by large motions errors or outliers.

**2.1.3. Image Model** In general, super-resolution is an ill-posed problem[2] either because it has infinite possible solutions or because it has great sensitivity to the noise [18, 3, 26]. In order to solve this problem and to obtain a unique and stable solution, most super-resolution algorithms exploit additional information about the desired images.

The additional information most commonly used is to assume that the images are smooth, which implies that the intensity variations of $\mathbf{f}_k$ are relatively small [6, 22]. This additional information is, in general, expressed as a side penalty of the form:

$$\frac{\mathcal{D}(\mathbf{R}_k \mathbf{f}_k)}{\beta_R} \tag{3}$$

1 The name *outlier* in the literature of statistics is a bad element or measure, usually of large magnitude, that does not follow the underlying statistical assumption [14].

2 An ill-posed problem is a mathematical problem that has, at least, one of the following features: it has no solution; it has an infinite number of solutions; or the solution is not stable due to small perturbations in the data [26, 10].

where $\mathcal{D}(\mathbf{x})$ is a chosen penalty and $\beta_R$ is the hyperparameter, related to the standard deviation. The matrix $\mathbf{R}_k$, of size $P \times M$, represents a discrete differential operator, either employing a finite difference operator (in the horizontal, vertical and diagonals directions) or a Laplacian operator. The resulting vector of $\mathbf{R}_k\mathbf{f}_k$ emphasizes the intensity variations of $\mathbf{f}_k$. Usually, the same operator is considered for all images in the sequence.

In this work it is considered the squared $\ell_2$ norm as a chosen penalty, where $\mathcal{D}(\mathbf{x}) = \|\mathbf{x}\|_2^2 = \sum_i |x_i|^2$. This norm helps to estimate smooth images and provides a resulting optimization algorithm with relatively low computational complexity. Many works [22, 23, 5] indicate the preference for images with sharp edges. The Huber norm, as well as the $\ell_1$ norm, are able to better preserve the edges of the estimated HR frames, in contrast to the $\ell_2$ norm. However, the determination of the correct parameter utilizing these norms is a more difficult problem and will not be addressed here. This paper focus on methods for determining the hyperparameter $\beta_R$ associated with the squared $\ell_2$ norm only.

### 2.2. Simultaneous SR Methods with Fixed Regularization Parameters

The simultaneous algorithms estimate the entire sequence of HR frames in a single process. This approach allows the inclusion of the motion matrix in the prior term, improving the quality of the estimated image sequence. The simultaneous approach was originally proposed in [4], and improved in [28, 29, 30] where the computational cost was reduced by removing the terms with the combined acquisition and motion matrix from the data term. The minimization problem, according to [30], is

$$\hat{\mathbf{f}}_1, \ldots, \hat{\mathbf{f}}_L = \arg\min_{\mathbf{f}_1,\ldots,\mathbf{f}_L} \sum_{k=1}^{L} \|\mathbf{g}_k - \mathbf{D}_k\mathbf{f}_k\|_2^2 + \lambda_R \sum_{k=1}^{L} \|\mathbf{R}_k\mathbf{f}_k\|_2^2 + \lambda_M \sum_{k=1}^{L-1} \|\mathbf{f}_k - \mathbf{M}_{k,k+1}\mathbf{f}_{k+1}\|_2^2 \quad (4)$$

where the sum of $\|\mathbf{g}_k - \mathbf{D}_k\mathbf{f}_k\|_2^2$ composes the data term, which enforces the similarity between the estimated sequence and the captured data. The prior term has two components: the component $\|\mathbf{R}_k\mathbf{f}_k\|_2^2$ enforces the images to be smooth, which is based on the image model; the component $\|\mathbf{f}_k - \mathbf{M}_{k,k+1}\mathbf{f}_{k+1}\|_2^2$ enforces the images to be similar, minimizing the finite difference in the motion trajectory, which is based on the motion model. The regularization parameters, $\lambda_R$ and $\lambda_M$, dictates the influence of each prior term in the solution. This regularized method is also the same deduced from the MAP estimative, as will be shown in Section 3.

Note that in (4) the entire HR sequence is estimated simultaneously, where only the acquisition matrix $\mathbf{D}_k$ is utilized in the data term [30]. In traditional SR methods, the frames are estimated one-by-one (non-simultaneously) and the data term includes a system which combines the motion model and the acquisition model. Moreover, whereas a first order finite difference model is used for the priors in (4), a second or arbitrary order models can also be used [30].

Equation (4) can be rewritten as

$$\hat{\boldsymbol{f}} = \arg\min_{\boldsymbol{f}} \|\boldsymbol{g} - \boldsymbol{D}\boldsymbol{f}\|_2^2 + \lambda_R\|\boldsymbol{R}\boldsymbol{f}\|_2^2 + \lambda_M\|\boldsymbol{M}\boldsymbol{f}\|_2^2 \quad (5)$$

where $\boldsymbol{g} = [\mathbf{g}_1^T \ldots \mathbf{g}_L^T]^T$ is the LR sequence, $\boldsymbol{f} = [\mathbf{f}_1^T \ldots \mathbf{f}_L^T]^T$ is the HR sequence, $\boldsymbol{D}$, $\boldsymbol{R}$ are block diagonals defined by $\boldsymbol{D} = \operatorname{diag}(\mathbf{D}_1, \cdots, \mathbf{D}_L)$ and $\boldsymbol{R} = \operatorname{diag}(\mathbf{R}_1, \cdots, \mathbf{R}_L)$, and

$$\boldsymbol{M} = \begin{bmatrix} \mathbf{I} & -\mathbf{M}_{1,2} & \cdots & \mathbf{0} \\ \vdots & \ddots & \ddots & \vdots \\ \mathbf{0} & \cdots & \mathbf{I} & -\mathbf{M}_{L-1,L} \end{bmatrix} \quad (6)$$

for the first order motion difference, as used in (4), where $\mathbf{I}$ is the identity matrix.

Note that the parameters $\lambda_R$ and $\lambda_M$ are assumed to be known and fixed values in (4) and (5). Since different values for the parameters lead to different resulting HR images, in order to be successful, the estimation process in (4), or (5), require proper values for these parameters, which are usually unknown in practical problems. This paper presents a new method to address the joint estimation of these parameters with the HR images.

## 3. Proposed Automatic Determination of the Regularization Parameters

This section describes the proposed approach to estimate the parameters based on the joint maximum a posteriori (JMAP) estimation. JMAP is a Bayesian estimator that focus on the estimation of the HR images and the parameters together [8].

### 3.1. Classical JMAP

The general JMAP estimative is given as:

$$\hat{\boldsymbol{f}}, \hat{\theta}, \hat{\beta}_R, \hat{\beta}_M = \arg\max_{\boldsymbol{f},\theta,\beta_R,\beta_M} \rho(\boldsymbol{f}, \theta, \beta_R, \beta_M|\boldsymbol{g}) \quad (7)$$

where $\rho(\boldsymbol{f}, \theta, \beta_R, \beta_M, |\boldsymbol{g})$ is the posterior density, $\boldsymbol{g}$ are the LR images, $\boldsymbol{f}$ are the HR images, $\theta$, is the data hyperparameter, and $\beta_R$ and $\beta_M$ are the hyperparameters of the image sequence prior density, and

$$\rho(\boldsymbol{f}, \theta, \beta_R, \beta_M|\boldsymbol{g}) \propto \rho(\boldsymbol{g}|\boldsymbol{f}, \theta)\rho(\theta)\rho(\boldsymbol{f}|\beta_R, \beta_M)\rho(\beta_R, \beta_M) \quad (8)$$

Functions $\rho(\theta)$, $\rho(\beta_R)$ and $\rho(\beta_M)$ are the prior densities assigned to the hyperparameters, also known as hyperpriors [8]. The data density, $\rho(\boldsymbol{g}|\boldsymbol{f},\theta)$, and the image prior density, $\rho(\boldsymbol{f}|\beta_R,\beta_M)$, are the same as used in MAP estimation. Let us assume the following Gaussian densities

$$\rho(\boldsymbol{g}|\boldsymbol{f},\theta) = \frac{(2\pi)^{-LN/2}}{(\theta)^{LN/2}} e^{-\frac{1}{2}\frac{\|\boldsymbol{g}-\boldsymbol{D}\boldsymbol{f}\|_2^2}{\theta}} \tag{9}$$

where $\theta$, in this case, is the variance of the acquisition noise in the data, $\sigma^2_{\boldsymbol{\eta}}$, assumed in (1) and

$$\rho(\boldsymbol{f}|\beta_R,\beta_M) \propto \frac{(2\pi)^{-LM/2}}{{\beta_R}^r {\beta_M}^m} e^{-\frac{1}{2}\left[\frac{\|\boldsymbol{R}\boldsymbol{f}\|_2^2}{\beta_R} + \frac{\|\boldsymbol{M}\boldsymbol{f}\|_2^2}{\beta_M}\right]} \tag{10}$$

where $r = \alpha \cdot rank(\boldsymbol{R})$, $m = \alpha \cdot rank(\boldsymbol{M})$, considering that $rank(\boldsymbol{R}) + rank(\boldsymbol{M}) \geq LM$, we have $\alpha = LM/[rank(\boldsymbol{R}) + rank(\boldsymbol{M})]$. In this work $\theta$ is assumed independent of $\beta_R$ and $\beta_M$. Observe that, according to (10), $\beta_R$ is related to the image smoothness, from the image model in (3), and $\beta_M$ is related to the images similarity in the motion trajectory, from the motion model in (2).

In MAP estimation the hyperparameters are assumed to have fixed values [8, 17], leading to (5), whereas in JMAP estimation, the hyperparameters are random values that need to be estimated from the data as well as the HR image. Thus, in the same way that an image prior is needed for the estimation of the HR image, the hyperpriors are needed for the estimation of the hyperparameters.

The classical JMAP assumes uniform densities for the hyperpriors as in [8, 17], where the values are equiprobable, therefore $\rho(\theta) \propto cte$ and $\rho(\beta_R,\beta_M) \propto cte$, for $0 < \theta, \beta_R, \beta_M < \infty$. The JMAP estimation with these hyperpriors becomes:

$$\hat{\boldsymbol{f}}, \hat{\theta}, \hat{\beta}_R, \hat{\beta}_M = \arg \min_{\boldsymbol{f},\theta,\beta_R,\beta_M} \frac{\|\boldsymbol{g}-\boldsymbol{D}\boldsymbol{f}\|_2^2}{2\theta} + \frac{LN}{2}\ln\theta + \frac{\|\boldsymbol{R}\boldsymbol{f}\|_2^2}{2\beta_R} + \frac{r}{2}\ln\beta_R + \frac{\|\boldsymbol{M}\boldsymbol{f}\|_2^2}{2\beta_M} + \frac{m}{2}\ln\beta_M + cte \tag{11}$$

From (11) it is possible to find the hyperparameters for a fixed $\boldsymbol{f}$, differentiating (11) with respect to the hyperparameters and setting the result to zero. This leads to the following closed form solutions:

$$\hat{\theta} = \frac{\|\boldsymbol{g}-\boldsymbol{D}\boldsymbol{f}\|_2^2}{LN}, \quad \hat{\beta}_R = \frac{\|\boldsymbol{R}\boldsymbol{f}\|_2^2}{r}, \qquad \hat{\beta}_M = \frac{\|\boldsymbol{M}\boldsymbol{f}\|_2^2}{m}. \tag{12}$$

for the data hyperparameter and for the image sequence hyperparameters, respectively. By substituting (12) into equation (11), leads to:

$$\hat{\boldsymbol{f}} = \arg\min_{\boldsymbol{f}} \ln(\|\boldsymbol{g}-\boldsymbol{D}\boldsymbol{f}\|_2^2) + \frac{r}{LN}\ln(\|\boldsymbol{R}\boldsymbol{f}\|_2^2) + \frac{m}{LN}\ln(\|\boldsymbol{M}\boldsymbol{f}\|_2^2) \tag{13}$$

The minimizer in (13) is shown to be the solution of

$$\left(\boldsymbol{D}^T\boldsymbol{D} + \lambda_R\boldsymbol{R}^T\boldsymbol{R} + \lambda_M\boldsymbol{M}^T\boldsymbol{M}\right)\boldsymbol{f} = \boldsymbol{D}^T\boldsymbol{g} \tag{14}$$

where $\lambda_R$ and $\lambda_M$ are:

$$\lambda_R = \frac{r}{LN}\frac{\|\boldsymbol{g}-\boldsymbol{D}\boldsymbol{f}\|_2^2}{\|\boldsymbol{R}\boldsymbol{f}\|_2^2}, \quad \lambda_M = \frac{m}{LN}\frac{\|\boldsymbol{g}-\boldsymbol{D}\boldsymbol{f}\|_2^2}{\|\boldsymbol{M}\boldsymbol{f}\|_2^2} \tag{15}$$

The cost function in (13) is non-convex[3] and the estimation unstable [17]. It requires proper constraining to avoid divergence. In the Bayesian statistical sense, constraints can be expressed by defining proper hyperparameter priors [8]. When employing uniform densities, as done in the classical JMAP, the hyperparameters are not properly constrained and generate unstable estimates. More restrictive hyperpriors, on the other hand, lead to a stable estimative and a globally convex problem with a unique minimum.

## 3.2. Proposed Method

The instability of the classical JMAP estimative, according to (13), is reported in [16, 15]. An approach to stabilize JMAP by employing a proper hyperprior for general inverse problems is reported in [7]. This work proposes an alternative hyperprior which is able to lead the JMAP to a unique and stable estimative of the parameters.

In the JMAP method, the density of the data or the prior density of the images is connected with the density of its respective hyperparameter. For example, consider only the use of the smoothness prior, $\rho(\boldsymbol{f}|\beta_R)$, which enforces the HR images to be smooth. The associated hyperparameter, $\beta_R$, defines "how smooth" is the resulting image. However, when an uniform density is assigned to the hyperparameter, as $\rho(\beta_R) \propto cte$, then it is implicitly assumed that an oversmooth image, like a constant intensity value image, when $\beta_R \to 0$, is as likely to occur as a noisy image, like the one produced by a completely unregularized estimation, when $\beta_R \to \infty$. The other extreme choice for the hyperparameter prior is to assume $\rho(\beta_R)$ as a Dirac delta function, i.e., an impulse in a fixed value for $\beta_R$, which leads (7) to (5). This choice is the most possible constraining for the hyperparameters.

3 Since the logarithm operator is a non-convex operator, so is a sum of logarithms.

Therefore, a proper hyperprior density should be found between the uniform and the delta density. It should prevent the hyperparameter to reach very extreme values, but it must allow them to fluctuate among a range of candidate values. Moreover, the desired prior density for the hyperparameters needs to enforce positive values and provide low probability for very low or very high values.

Among several candidates, the gamma density, with specific designed parameters to make it similar to the chi-squared density, has been shown practical and theoretical advantages over the alternatives. The gamma densities for the hyperparameters are given by

$$\rho(\theta) = \frac{\theta^{(a-1)} b^{-a}}{\Gamma(a)} e^{-\dfrac{\theta}{b}} \tag{16}$$

$$\rho(\beta_R, \beta_M) = \frac{\beta_R^{(c-1)} \beta_M^{(h-1)} d^{-c} i^{-h}}{\Gamma(c)\Gamma(h)} e^{-\left[\dfrac{\beta_R}{d} + \dfrac{\beta_M}{i}\right]} \tag{17}$$

where $a$, $c$ and $h$ are the scale factors, $b$, $d$ and $i$ are the shape factors, and $\Gamma(x)$ is the gamma function. Also, $E\{\theta\} = ab$, $\text{var}\{\theta\} = ab^2$, $E\{\beta_R\} = cd$ and $\text{var}\{\beta_R\} = cd^2$, and $E\{\beta_M\} = hi$ and $\text{var}\{\beta_M\} = hi^2$.

Substituting the gamma densities in equation (7) leads to:

$$\begin{aligned}\hat{\boldsymbol{f}}, \hat{\theta}, \hat{\beta}_R, \hat{\beta}_M = &\arg\min_{\boldsymbol{f},\theta,\beta_R,\beta_M} \frac{\|\boldsymbol{g}-\boldsymbol{D}\boldsymbol{f}\|_2^2}{2\theta} + \left(\frac{LN}{2} - a + 1\right)\ln\theta \\ &+ \frac{\theta}{b} + \frac{\|\boldsymbol{R}\boldsymbol{f}\|_2^2}{2\beta_R} + \left(\frac{r}{2} - c + 1\right)\ln\beta_R + \frac{\beta_R}{d} \\ &+ \frac{\|\boldsymbol{M}\boldsymbol{f}\|_2^2}{2\beta_M} + \left(\frac{m}{2} - h + 1\right)\ln\beta_M + \frac{\beta_M}{i} + cte\end{aligned} \tag{18}$$

Note that when $a = LN/2 + 1$, $c = r/2 + 1$ and $h = m/2 + 1$, the gamma density has nearly the same shape as the chi-squared density. These values for $a$, $c$ and $h$ will be used in our development, they provide a necessary condition to achieve a globally convex problem. The $b$, $d$ and $i$ will be replaced by expressions involving the expected values of the hyperparameters, namely $b = E\{\theta\}/a = m_\theta/a$, $d = E\{\beta_R\}/c = m_{\beta_R}/c$, and $i = E\{\beta_M\}/h = m_{\beta_M}/h$. Assigning the mentioned values for $a$, $b$, $c$, $d$, $h$, and $i$, and applying some algebra, equation (18) reduces to:

$$\begin{aligned}\hat{\boldsymbol{f}}, \hat{\theta}, \hat{\beta}_R, \hat{\beta}_M = &\arg\min_{\boldsymbol{f},\theta,\beta_R,\beta_M} \frac{\|\boldsymbol{g}-\boldsymbol{D}\boldsymbol{f}\|_2^2}{2\theta} + \frac{\theta(LN+2)}{2m_\theta} \\ &+ \frac{\|\boldsymbol{R}\boldsymbol{f}\|_2^2}{2\beta_R} + \frac{\beta_R(r+2)}{2m_{\beta_R}} + \frac{\|\boldsymbol{M}\boldsymbol{f}\|_2^2}{2\beta_M} + \frac{\beta_M(m+2)}{2m_{\beta_M}}\end{aligned} \tag{19}$$

Differentiating equation (19) with respect to the hyperparameters, for fixed $\boldsymbol{f}$, leads to the following estimative

$$\begin{aligned}&\hat{\theta} = \frac{\sqrt{m_\theta}\|\boldsymbol{g}-\boldsymbol{D}\boldsymbol{f}\|_2}{\sqrt{LN+2}}, \\ &\hat{\beta}_R = \frac{\sqrt{m_{\beta_R}}\|\boldsymbol{R}\boldsymbol{f}\|_2}{\sqrt{r+2}}, \quad \hat{\beta}_M = \frac{\sqrt{m_{\beta_M}}\|\boldsymbol{M}\boldsymbol{f}\|_2}{\sqrt{m+2}}.\end{aligned} \tag{20}$$

Substituting the results in (20) into (19), gives

$$\hat{\boldsymbol{f}} = \arg\min_{\boldsymbol{f}} \|\boldsymbol{g} - \boldsymbol{D}\boldsymbol{f}\|_2 + \mu_R\|\boldsymbol{R}\boldsymbol{f}\|_2 + \mu_M\|\boldsymbol{M}\boldsymbol{f}\|_2 \tag{21}$$

where

$$\begin{aligned}\mu_R &= \sqrt{\frac{m_\theta(r+2)}{m_{\beta_R}(LN+2)}}, \\ \mu_M &= \sqrt{\frac{m_\theta(m+2)}{m_{\beta_M}(LN+2)}}\end{aligned} \tag{22}$$

Considering the gradient of the cost function in (21), the solution of this optimization problem is found when

$$\left(\boldsymbol{D}^T\boldsymbol{D} + \lambda_R\boldsymbol{R}^T\boldsymbol{R} + \lambda_M\boldsymbol{M}^T\boldsymbol{M}\right)\boldsymbol{f} = \boldsymbol{D}^T\boldsymbol{g} \tag{23}$$

where the parameters are defined by

$$\begin{aligned}\lambda_R &= \mu_R\frac{\|\boldsymbol{g} - \boldsymbol{D}\boldsymbol{f}\|_2}{\|\boldsymbol{R}\boldsymbol{f}\|_2}, \\ \lambda_M &= \mu_M\frac{\|\boldsymbol{g} - \boldsymbol{D}\boldsymbol{f}\|_2}{\|\boldsymbol{M}\boldsymbol{f}\|_2}\end{aligned} \tag{24}$$

The values of $\mu_R$ and $\mu_M$ can be chosen from average values, as in (22), or from an analysis of the estimation error which gives

$$\begin{aligned}\mu_R &= \frac{\sqrt{tr(\boldsymbol{D}^T\boldsymbol{D})}}{2\sqrt{tr(\boldsymbol{R}^T\boldsymbol{R})}}, \\ \mu_M &= \frac{\sqrt{tr(\boldsymbol{D}^T\boldsymbol{D})}}{2\sqrt{tr(\boldsymbol{M}^T\boldsymbol{M})}}\end{aligned} \tag{25}$$

The choice of these values, based on the estimation error, is addressed in [27].

The proposed method involves a convex[4] cost function with a unique minimum. In pracice, the HR image is computed by minimizing the cost function in (21) using the non-linear conjugated gradient (NL-CG) [26].

## 4. Experiments

The following experiment evaluates the performance of the simultaneous SR algorithms with known fixed parameters and with automatic determination of the parameters.

4 The $\ell_2$ norm is a convex operator.

Given a HR image sequence, with known or previously estimated motion, the simulated acquisition process was performed, employing the average of a squared area of $R \times R$ pixels using two subsampling factors $R = 2, 3$, and an additive white Gaussian noise with variance adjusted to achieve a fixed SNR [5]. Two situations were considered: high acquisition noise, with $\text{SNR}_A$=20dB and medium noise, with $\text{SNR}_A$=30dB. These noise levels are the typical levels found in commercial image sensors[6].

The quality of the HR sequence recovered with the tested methods is measured in terms of SNR. Computational effort of each method was evaluated by considering the time it takes for convergence, where convergence is assumed to be reached when the improvement in quality is less $10^{-2}$ dB.

This procedure was repeated using 20 random noisy realizations for each noise level. The entire experiment was repeated for each image sequence of a total of 6 different image sequences. In some of the sequences, the motion was artificially generated without considering occlusions in the scene, whereas in other sequences, which are from real video sequences, the motion was estimated using the optical flow method [13]. In this case, linear interpolated versions of the LR images were employed. The estimated motion vectors are not completely reliable in this case, therefore, occlusions and motion errors occur in several places in the sequence.

In this evaluation, the procedure of detection and removal of the occlusion regions was not considered in order to evaluate the performance of the methods in controlling the similarity of the images.

The following methods were compared:

**JMAP** - The classical JMAP approach [8] as equation (13), using conjugate gradient method to find the HR images with (12) to update the parameters.

**PROP** - Proposed method with minimization using GC-NL.

These methods are iterative. The same initial conditions are considered: the initial HR image is a null image, and the initial parameters is randomly chosen from $10^{-6}$ to $10^{6}$. In addition to these methods, the results obtained by the following pre-determined parameter were also compared:

**KNOWN** - Employs the MAP estimative where the parameters are known a priori. Since the noise and the original HR images are known in the experiments, the hyperparameters are computed without difficulties. This method is used as reference only. It cannot be used in practice since neither the parameters nor the HR images are known a priori.

5 The acquisition SNR is defined as $\text{SNR}_A = 10\log_{10}(\sigma^2_{\boldsymbol{Df}}/\sigma^2_{\boldsymbol{\eta}})$, where $\sigma^2_{\boldsymbol{Df}}$ is a LR noise free sequence variance and $\sigma^2_{\boldsymbol{\eta}}$ is the noise variance.

6 Typical acquisition SNR may vary from 10dB to 40dB, depending on the exposure.

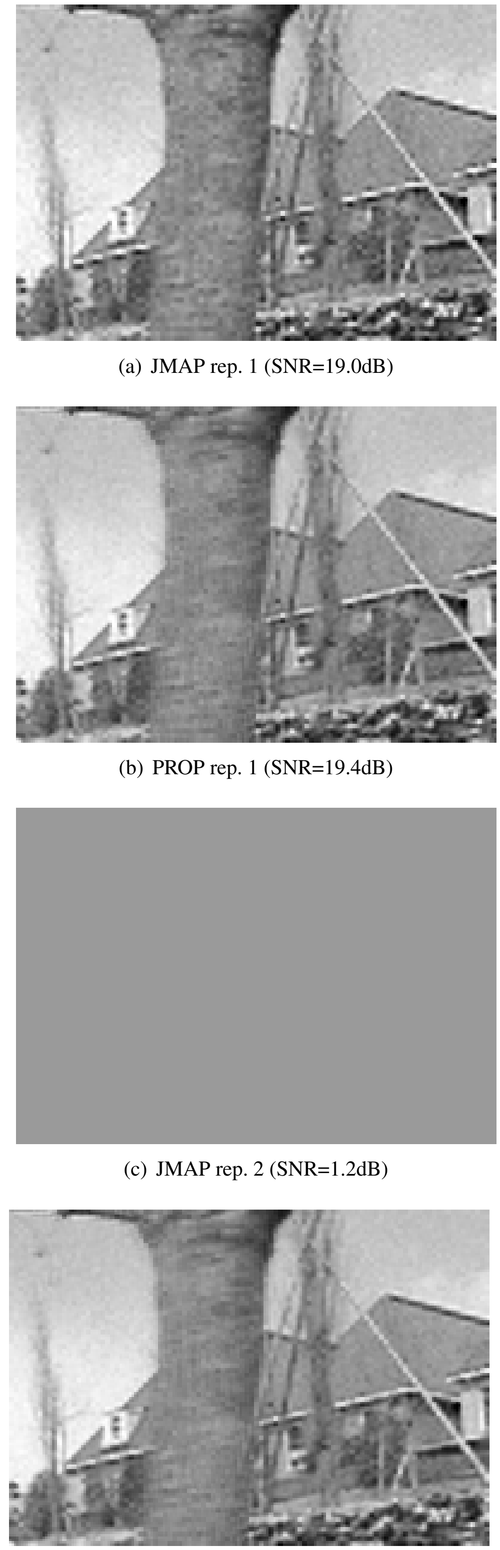

(a) JMAP rep. 1 (SNR=19.0dB)

(b) PROP rep. 1 (SNR=19.4dB)

(c) JMAP rep. 2 (SNR=1.2dB)

(d) PROP rep. 2 (SNR=19.8dB)

**Figure 1. Visual results comparing Classical JMAP and the proposed method in two different repetitions.**

| Method | $R$=2 SNR$_A$=20dB | | | $R$=3 SNR$_A$=30dB | | |
|---|---|---|---|---|---|---|
| | SNR | STD | CT | SNR | STD | CT |
| JMAP | 22.6 | 1.1 | 5.8 | 20.0 | 2.2 | 8.1 |
| KNOWN | 22.1 | 0.4 | 1.0 | 20.8 | 1.2 | 1.0 |
| PROP | 23.1 | 0.4 | 1.3 | 21.2 | 2.0 | 3.1 |

**Table 1. SNR average in dB, standard deviation (STD), and relative computational time (CT) for simultaneous SR algorithms**

The average quality of the estimated images with the parameters found by the respective method, its standard deviation, and the relative computational time (with respect to KNOWN) are shown in Table 1. One can observe in Table 1 that the quality obtained by the proposed method was superior to the obtained by KNOWN and JMAP. Moreover, the results illustrate the low computational cost provided by the proposed method, which is faster than the classical JMAP. Unfortunately, up to now there is no other method to determine the parameters for the simultaneous SR methods in order to compare with the proposed method, except for the classical JMAP approach.

It is important to observe that the results provided by KNOWN are not necessarily the best results. One of the reasons for that in the modeling mismatches related to the gaussianity assumption for the motion error and spatial differences. An extensive search for the best parameters should be done in order to find them. However, this is a very time consuming task for more that one parameter in SR algorithms.

Figure 1 illustrates the instability of the JMAP. On can observe that in repetition 1 the JMAP converged to a good solution. However, in repetition 2 the JMAP estimation diverged to an image with constant intensity. This happened because the regularization parameter related to the image smoothness diverged toward infinity.

### 4.1. Example with Practical SR Algorithm

Figure 2 shows a result without artificial degradation and recovering, using $R = 3$. For this visual experiment, the original sequence is assumed to be the captured sequence and used as test problem for the simultaneous SR method with occlusion and motion error detection and removal [11] procedures. The enhancement of the resolution of the SR method over the original image can be clearly noticed. The regularization parameter was determined by the proposed method.

(a) Image at original resolution

(b) Nearest neighbor (3X) interpolation of the original image

(c) Super resolution with the proposed approach

**Figure 2. Visual results comparing the original frame of the sequence Flower Garden with the same frame, where a resolution improvement factor of $R$=3 was applied.**

## 5. Conclusions

In this paper, a novel regularized simultaneous super-resolution technique with automatic determination of the parameter is proposed. The problem of parameters and image sequence estimation has been addressed with the Bayesian theory, using joint maximum a posteriori (JMAP) estimation. A gamma density is proposed for the hyperparameters in order to provide a globally convex cost function, resulting in a unique solution. The proposed method provides a computational cost similar to the method with fixed parameters. We provide a set of experiments to illustrate the superior efficiency and stability of the proposed technique when compared with other competing methods.

## References


[1] H. H. Barrett and K. J. Myers. *Foundations of Image Science*. Wiley Series in Pure and Applied Optics. John Wiley & Sons, 2004.

[2] S. Borman and R. Stevenson. Linear models for multi-frame super-resolution restoration under non-affine registration and spatially varying psf. In *SPIE Electronic Imaging*, Jan. 2004.

[3] S. Borman and R. L. Stevenson. Spatial resolution enhancement of low-resolution image sequences. a comprehensive review with directions for future research. Technical report, University of Notre Dame, 1998.

[4] S. Borman and R. L. Stevenson. Simultaneous multi-frame map super-resolution video enhancement using spatio-temporal priors. In *IEEE International Conference on Image Processing*, volume 3, pages 469–473, Oct. 1999.

[5] C. Bouman and K. Sauer. A generalized gaussian image model for edge-preserving map estimation. *IEEE Transactions on Image Processing*, 2(3):269–310, July 1993.

[6] A. Bovik, editor. *Handbook of Image and Video Processing*. Academic Press, 2000.

[7] A. M. Djafari. A full bayesian approach for inverse problems. In *15th Int. Work. on Max. Entropy and Bayesian Meth.*, 1995.

[8] A. M. Djafari. Joint estimation of parameters and hyperparameters in a bayesian approach of solving inverse problems. In *IEEE Int. Conf. on Image Proc.*, pages 473–472, Sept. 1996.

[9] S. Farsiu, D. Robinson, M. Elad, and P. Milanfar. Fast and robust multi-frame super-resolution. *IEEE Trans. on Image Proc.*, 13(10):1327–1344, Oct. 2004.

[10] P. C. Hansen, editor. *Rank-Deficient and Discrete Ill-Posed Problems*. SIAM Monoghraphs an Matematical Modeling and Computation. SIAM, 1998.

[11] D. Hasler, L. Sbaiz, S. Süsstrunk, and M. Vetterli. Outlier modeling in image matching. *IEEE Trans. on Patt. Anal. and Mach. Intel.*, 25(3):301–315, Mar. 2003.

[12] M. C. Hong, M. G. Kang, and A. K. Katsaggelos. An iterative weighted regularized algorithm for improving the resolution of video sequences. In *IEEE International Conference on Image Processing*, volume 2, pages 474–477, Oct. 1997.

[13] B. K. P. Horn and B. G. Schunck. Determining optical flow. *Artif. Intel.*, 17:185–203, Aug. 1981.

[14] P. J. Huber. *Robust Statistics*. John Wiley & Sons, 1981.

[15] E. S. Lee and M. G. Kang. Regularized adaptive high-resolution image reconstruction considering inaccurate sub-pixel registration. *IEEE Trans. on Image Proc.*, 12(7):826–837, July 2003.

[16] R. Molina, A. K. Katsaggelos, and J. Mateos. Bayesian and regularization methods for hyperparameter estimation in image restoration. *IEEE Transactions on Image Processing*, 8(2):231–246, Feb. 1999.

[17] R. Molina, M. Vega, J. Abad, and A. K. Katsaggelos. Parameter estimation in bayesian high-resolution image reconstruction with multisensors. *IEEE Trans. on Image Proc.*, 12(12):1655–1667, Dec. 2003.

[18] S. C. Park, M. K. Park, and M. G. Kang. Super-resolution image reconstruction: a technical overview. *IEEE Signal Processing Magazine*, 20(3):21–36, May 2003.

[19] Y. Saad. *Iterative methods for sparse linear systems*. International Thompson Publishing, 1995.

[20] R. R. Schultz, L. Meng, and R. L. Stevenson. Subpixel motion estimation for super-resolution image sequence enhancement. *Journal of Visual Communication and Image Representation*, 9(1):38–50, Mar. 1998.

[21] R. R. Schultz and R. L. Stevenson. Extraction of high-resolution frames from video sequences. *IEEE Trans. on Image Proc.*, 5(6):996–1011, June 1996.

[22] A. Srivastava. Stochastic models for capturing image variability. *IEEE Signal Processing Magazine*, 19(5):63–76, Sept. 2002.

[23] R. L. Stevenson, B. E. Schmitz, and E. J. Delp. Discontinuity preserving regularization of inverse visual problems. *IEEE Transactions on Systems, Man and Cybernetics*, 24(3):455–469, Mar. 1994.

[24] C. Stiller and J. Konrad. Estimating motion in image sequences. *IEEE Signal Proc. Magazine*, 16(4):70–91, July 1999.

[25] R. Y. Tsai and T. S. Huang. Multiframe image restoration and registration. *Advances in Comp. Vision and Image Proc.*, 1:317–339, 1984.

[26] C. R. Vogel. *Computational Methods for Inverse Problems*. Frontiers in Applied Mathematics. SIAM, 2002.

[27] M. V. W. Zibetti, F. S. V. Bazán, and J. Mayer. Determining the regularization parameters for super-resolution problems. *accepted for publication in Elsevier - Signal Processing*, June 2008.

[28] M. V. W. Zibetti and J. Mayer. Simultaneous super-resolution for video sequences. In *IEEE International Conference on Image Processing*, volume 1, pages 877–880, Sept. 2005.

[29] M. V. W. Zibetti and J. Mayer. Outlier robust and edge-preserving simultaneous super-resolution. In *IEEE International Conference on Image Processing*, volume 1, pages 1741–1744, Oct. 2006.

[30] M. V. W. Zibetti and J. Mayer. A robust and computationally efficient simultaneous super-resolution scheme for image sequences. *IEEE Transactions on Circuits and Systems for Video Technology*, 17(10):1288–1300, Oct. 2007.